



UNIVERSITI PUTRA MALAYSIA

**PREPARATION AND CHARACTERIZATION OF NATURAL
RUBBER/CLAY, POLY(ETHYLENE-CO-VINYL ACETATE)/CLAY AND
NATURAL RUBBER/POLY(ETHYLENE-CO-VINYL ACETATE)/CLAY
NANOCOMPOSITES**

JAMALIAH BT SHARIF

FS 2005 14

**PREPARATION AND CHARACTERIZATION OF NATURAL
RUBBER/CLAY, POLY(ETHYLENE-CO-VINYL ACETATE)/CLAY AND
NATURAL RUBBER/POLY(ETHYLENE-CO-VINYL ACETATE)/CLAY
NANOCOMPOSITES**

By

JAMALIAH BT SHARIF

**Thesis Submitted to the School of Graduate Studies, Universiti Putra Malaysia,
in Fulfilment of the Requirements for the Degree of Doctor of Philosophy**

October 2005



DEDICATED TO

**My beloved family
Hubby: Mohd Mustafah
Daughters: Dr Nadia and Syaza
Sons: Yasir, Anas, Farid and Hilmi
Daughter inlaw: Amelia
For their prayers and
moral support**

Abstract of thesis presented to the Senate of Universiti Putra Malaysia in fulfilment of the requirements for the degree of Doctor of Philosophy

PREPARATION AND CHARACTERIZATION OF NATURAL RUBBER/CLAY, POLY(ETHYLENE-CO-VINYL ACETATE)/CLAY AND NATURAL RUBBER /POLY(ETHYLENE-CO-VINYL ACETATE)/CLAY NANOCOMPOSITES

By

JAMALIAH BT SHARIF

October 2005

Chairman: Professor Wan Md Zin Wan Yunus, PhD

Faculty: Science

This thesis describes the preparation, characterization and physicochemical properties of natural rubber/clay, poly(ethylene-co-vinyl acetate)/clay and natural rubber /poly(ethylene-co-vinyl acetate)/clay nanocomposites.

In order to improve the clay and polymer compatibility, the clay was first converted into the organoclay. The organoclays were prepared from sodium montmorillonite (Na-MMT) through cation exchange reaction using cetyltrimethyl ammonium bromide, octadecyl ammonium chloride or dodecyl ammonium chloride. The x-ray diffraction (XRD) results reveal that the interlayer distance of the Na-MMT increases with the formation of the organoclays. The presence of the alkyl ammonium ions in the organoclays was also studied by the Fourier transforms infrared spectroscopy (FTIR). The amount of alkyl ammonium ions intercalated into the clay galleries increases with the increase of alkyl ammonium chain length as shown by elemental analysis and thermogravimetric analysis (TGA) results.

The nanocomposites were prepared by melt blending the natural rubber (NR), poly (ethylene-co-vinyl acetate) (EVA) or blend of both NR and EVA with the organoclays. The compounds were then crosslinked with an electron beam (EB) irradiation. The XRD patterns showed that all of the nanocomposites produced from this work are of intercalated-type. These were further confirmed by transmission electron microscopy (TEM) observation. Scanning electron microscopy (SEM) study on the cryo-fractured surface reveals that the pure Na-MMT dispersed in the polymer matrix in large agglomerated form while the modified Na-MMT separated into small aggregates and dispersed homogeneously in the polymer matrix.

The optimum irradiation dose for crosslinking of NR, EVA and NR/EVA nanocomposites was determined. The formation of radiation induced crosslinking in NR, EVA and NR/EVA blend was not inhibited with the presence of dodecyl ammonium montmorillonite (DDA-MMT) but it was affected by the presence of dimethyl dehydrogenated tallow montmorillonite (C20A). The tensile modulus of all the nanocomposites increases with the increase of the clay content of up to 10 phr. The tensile strength and elongation at break of the NR/clay nanocomposites increases with the increase of organoclays up to 3 phr and decreases with further increase of the organoclay content. However, the tensile strength of EVA/clay and NR/EVA/clay nanocomposites remains constant with the increase of the organoclay content of up to 5 phr but decreases with the increase of organoclay content of up to 10 phr. The elongation at break of both EVA/clay and NR/EVA/clay decreases slightly with the increase of organoclay content. Electron beam irradiation of the nanocomposites increases the tensile modulus and tensile strength further but decreased the elongation at break.

The dynamic storage modulus of all nanocomposites increases with the increase of organoclay concentration in the investigated temperature range. The shifting of the glass transition temperature (T_g) indicates improved adhesion between the polymer matrix and the clay layers. TGA analysis reveals that the nanocomposites undergo slower thermal degradation than that of the pure polymer or conventional composite of the polymer with unmodified sodium montmorillonite. The decomposition temperature of the nanocomposites increase with the increase of organoclay content of up to 5 phr and beyond that the decomposition temperature remains constant or decreases.

Abstrak tesis yang dikemukakan kepada Senat Universiti Putra Malaysia sebagai memenuhi keperluan untuk ijazah Doktor Falsafah

**PENYEDIAAN DAN PENCIRIAN NANOKOMPOSIT GETAH ASLI/
TANAH LIAT, POLI(ETILENA-KO-VINIL ASETAT)/TANAH LIAT
DAN NANOKOMPOSIT GETAH ASLI/ POLI(ETILENA-KO-VINIL
ASETAT)/TANAH LIAT**

Oleh

JAMALIAH BT SHARIF

Oktober 2005

Pengerusi: Professor Wan Md Zin Wan Yunus, PhD

Fakulti: Sains

Tesis ini menerangkan penyediaan, pencirian dan sifat kimia dan fizik nanokomposit getah asli/tanah liat, poli(etilena-ko-vinil asetat)/tanah liat dan getah asli/poli(etilena-ko-vinil asetat)/tanah liat.

Untuk meningkatkan keserasian pengadunan tanah liat dengan polimer, tanah liat diubahsuai terlebih dahulu kepada organo-tanah liat. Organo-tanah liat disediakan daripada sodium montmorillonit (Na-MMT) melalui tindak balas penukar kation menggunakan cetiltrimetil ammonium bromida, oktadesil ammonium klorida atau dodesil ammonium klorida. Keputusan belauan sinar-x (XRD) menunjukkan jarak antara lapisan Na-MMT bertambah dengan pembentukan organo-tanah liat. Kehadiran ion alkil ammonium dalam organo-tanah liat juga ditentukan dengan menggunakan spektroskopi infra-merah pengubah Fourier (FTIR). Jumlah ion alkil ammonium yang termasuk ke dalam lapisan tanah liat bertambah dengan pertambahan

panjang rantai alkil ammonium seperti yang ditunjukkan oleh keputusan analisis unsur dan analisis termogravimetri (TGA).

Nanokomposit telah disediakan daripada getah asli (NR), poli(etilena-ko-vinil asetat) (EVA) dan adunan NR dan EVA melalui pengadunan leburan dengan organo-tanah liat. Sebatian telah ditautsilang dengan sinaran alur elektron. Keputusan XRD menunjukkan bahawa semua nanokomposit yang dihasilkan daripada kerja ini adalah daripada jenis 'intercalated'. Keputusan ini seterusnya disokong oleh pemerhatian mikroskop transmisi elektron (TEM). Kajian mikroskop imbasan elektron (SEM) ke atas permukaan sampel kriopatahan menunjukkan Na-MMT berselerak di dalam matrik polimer dalam bentuk agglomerat (gabungan aggregate kecil) yang besar manakala organo-tanah liat terpecah kepada agregat yang lebih kecil dan bertabur secara homogen di dalam matrik polimer.

Dos optima penyinaran untuk pembentukan tautsilang NR, EVA dan NR/EVA nanokomposit telah ditentukan. Kehadiran dodesil ammonium monmorilonit (DDA-MMT) didapati tidak merencat pembentukan tautsilang yang diaruh oleh sinaran tetapi terencat dengan kehadiran dimetil dihidrogenated tallow ammonium montmorillonit (C20A). Modulus tegangan bagi semua nanokomposit meningkat dengan peningkatan kandungan organo-tanah liat hingga 10 bps. Kekuatan tegangan dan pemanjangan pada takat putus bagi NR/tanah liat nanokomposit meningkat dengan peningkatan organo-tanah liat sehingga 3 phr dan menurun dengan penambahan organo-tanah liat sehingga 10 phr. Walau bagaimanapun bagi EVA/tanah liat dan NR/EVA/tanah liat nanokomposit, kekuatan tegangan tidak berubah dengan peningkatan organo-tanah liat sehingga 5 phr tetapi menurun dengan

peningkatan organo-tanah liat seterusnya. Pemanjangan pada takat putus menurun dengan peningkatan kandungan tanah liat. Penyinaran alur elektron ke atas nanokomposit telah meningkatkan lagi modulus tegangan dan kekuatan tegangan dan mengurangkan pemanjangan pada takat putus.

Modulus simpanan dinamik (G') bagi semua nanokomposit bertambah dengan pertambahan kandungan organo-tanah liat pada julat suhu kajian. Peningkatan pada suhu peralihan kaca (T_g) menunjukkan terdapat lekatan yang lebih baik di antara matrik polimer dengan lapisan tanah liat. Analisis termogravimetri menunjukkan nanokomposit menjalani degradasi lebih lambat berbanding polimer tulen atau komposit biasa antara polimer dan sodium montmorillonit yang tidak dirawat. Suhu penguraian nanokomposit meningkat dengan peningkatan kandungan organo-tanah liat sehingga 5 phr selepas takat ini suhu penguraian akan tetap atau menurun.

ACKNOWLEDGMENTS

First and foremost I would like to express my profound and most sincere gratitude to Prof Dr Wan Md Zin Wan Yunus chairman of the supervisory committee and to other members of the committee, Dr Khairul Zaman Hj Mohd Dahlan and Associate Prof Dr Mansor Hj Ahmad for their guidance, suggestions and continuous encouragement throughout the course of this work.

I would like to acknowledge the technical staff of Chemistry Department UPM, Mr Kamal, Mr Ismail and Mrs Rosnani for their help in getting the TGA, CHNS and FTIR data and Miss Azilah, Mr Ho, and Mr Rafi from microscopy and microanalysis unit UPM for their help in getting the TEM micrographs.

I am very grateful to Wan Ali, Zahid, Kamarolzaman, Rosli, Shari, Kamaruddin, Azmi, Ayub and Abdul Basit from BTPS, MINT for their assistance in irradiation and experimental work. Many thanks are due for Saiful and Zaiton from BTI, MINT for their help in getting the SEM micrographs. I am thankful to all my friends Dr Ishak, Dr Kamaruddin, Dr Zulkafli, Dr Dahlan, Norjanah, Aidil, Nor Azowa and Fadzlon for their help, advice and encouragement in completing this work.

I also indebted to the Malaysian Government and my employer, Malaysian Institute for Nuclear Technology Research (MINT), in particular, for sponsoring the work and for granting me the study leave. Finally, I would like to extend my sincere gratitude to my beloved husband Mohd Mustafah and my six wonderful childrens for being a constant source of encouragement and inspiration.

I certify that an Examination Committee met on 27th October 2005 to conduct the final examination of Jamaliah Sharif on her Doctor of Philosophy thesis entitled "Preparation and Characterization of Natural Rubber/Clay, Poly (Ethylene-Co-Vinyl Acetate)/Clay and Natural Rubber/Poly (Ethylene-Co-Vinyl Acetate)/Clay Nanocomposites" in accordance with Universiti Pertanian Malaysia (Higher Degree) Act 1980 and Universiti Pertanian Malaysia (Higher Degree) Regulations 1981. The Committee recommends that the candidate be awarded the relevant degree. Members of the Examination Committee are as follows:

ANUAR KASSIM, PhD

Professor
Faculty of Science
Universiti Putra Malaysia
(Chairman)

MOHAMAD ZAKI ABD RAHMAN, PhD


Associate Professor
Faculty of Science
Universiti Putra Malaysia
(Internal Examiner)

MOHD ZOBIR HUSSEIN, PhD

Professor
Faculty of Science
Universiti Putra Malaysia
(Internal Examiner)

HANAFI ISMAIL, PhD

Professor
School of Materials and Minerals Resources Engineering
Universiti Sains Malaysia
(External Examiner)


HASANAH MOHD. GHAZALI, PhD
Professor/Deputy Dean
School of Graduate Studies
Universiti Putra Malaysia

Date: **27 DEC 2005**

This thesis submitted to the Senate of Universiti Putra Malaysia and has been accepted as fulfilment of the requirements for the degree of Doctor of Philosophy. The members of the Supervisory Committee are as follows:

WAN MD ZIN WAN YUNUS, PhD

Professor
Faculty of Science
Universiti Putra Malaysia
(Chairman)

MANSOR AHMAD, PhD

Lecturer
Faculty of Science
Universiti Putra Malaysia
(Member)

KHAIRULZAMAN DAHLAN, PhD

Director of Radiation Processing Technology Division
Malaysian Institute for Nuclear Technology Research (MINT)
(Member)



AINI IDERIS, PhD
Professor/Dean
School of Graduate Studies
Universiti Putra Malaysia

Date: **12 JAN 2006**

DECLARATION

I hereby declare that the thesis is based on my original work except for quotations and citations, which have been duly acknowledged. I also declare that this thesis has not been previously or concurrently submitted for any other degree at UPM or any other institutions.



JAMALIAH BT SHARIF

Date: 26th DEC 2005

TABLE OF CONTENTS

	Page
DEDICATION	ii
ABSTRACT	iii
ABSTRAK	vi
ACKNOWLEDGMENTS	ix
APPROVAL SHEETS	x
DECLARATION FORM	xii
LIST OF TABLES	xvi
LIST OF FIGURES	xviii
LIST OF ABBREVIATIONS/NOTATIONS/GLOSSARY OF TERMS	xxiv
 CHAPTER	
 1 INTRODUCTION	 1
1.1 Background of the Study	1
1.2 Nanocomposite	4
1.3 Structure of Polymer Layered Silicate Nanocomposite	5
1.4 Natural Rubber	7
1.5 Poly(Ethylene-co-Vinyl Acetate)	8
1.6 Clay	9
1.7 Radiation Crosslinking of Polymers	13
1.8 Objectives of the Study	16
 2 LITERATURE REVIEW	 17
2.1 Preparation Methods of Nanocomposites	17
2.2 Intercalation of Polymer or Pre-polymer from Solution (Solution Blending)	18
2.3 In-situ Intercalative Polymerization	19
2.4 Melt Intercalation	22
2.5 Rubber/Clay Nanocomposites	28
2.6 Poly(Ethylene-co-Vinyl Acetate)/Clay Nanocomposites	31
2.7 Polymer Blend/Clay Nanocomposites	35
2.8 Properties of Nanocomposites	38
2.8.1 Tensile Properties	38
2.8.1.1 Tensile Modulus	38
2.8.1.2 Stress at Break	42
2.8.1.3 Elongation at Break	45
2.8.2 Dynamic Mechanical Analysis	47
2.8.3 Thermal Stability	50
2.8.4 Flame Retardancy	54
2.8.5 Gas Barrier Properties	57
 3 MATERIALS AND METHODS	 59
3.1 Materials	59
3.2 Preparation of Organoclays	60



3.3	Characterization of the Organoclays	61
3.3.1	X-ray Diffraction Study	61
3.3.2	Elemental Analysis	62
3.3.3	FTIR Spectroscopy	62
3.3.4	Thermogravimetric Analysis	62
3.4	Preparation of Nanocomposites via Melt Blending	63
3.4.1	Natural Rubber/Clay Nanocomposites	63
3.4.2	Poly(Ethylene-co-Vinyl Acetate)/Clay Nanocomposites	64
3.4.3	Natural Rubber/Poly(Ethylene-co-Vinyl Acetate)/Clay Nanocomposites	65
3.5	Irradiation of Samples	66
3.6	Characterization of Nanocomposites	66
3.6.1	X-ray Diffraction Study	66
3.6.2	Transmission Electron Microscopy	66
3.6.3	Scanning Electron Microscopy	67
3.6.4	Gel Content Measurement	67
3.6.5	Tensile Properties Measurement	68
3.6.6	Dynamic Mechanical Analysis	68
3.6.7	Thermogravimetric Analysis	69
3.6.8	Oxygen Index	69
4	RESULTS AND DISCUSSION	70
4.1	Preparation and Characterization of Organoclays	70
4.1.1	Interlayer Distance of Organoclays Determine by X-Ray Diffraction	70
4.1.2	Analysis of FTIR Spectra	72
4.1.3	Elemental Analysis	74
4.1.4	Thermogravimetric Analysis of Organoclays	74
4.2	Optimum Preparation Conditions of Natural Rubber/Clay Nanocomposites	78
4.2.1	Effect of Mixing Temperature on Clay Dispersion in the Natural Rubber matrix	78
4.2.2	Effect of Rotor Speed on Clay Dispersion in the Natural Rubber matrix	81
4.2.3	Effect of Mixing Time on Clay Dispersion in the Natural Rubber matrix	83
4.3	Characterization of Natural Rubber/Clay Nanocomposites	85
4.3.1	X-Ray Diffraction Study	85
4.3.2	Morphology Study by TEM	91
4.3.3	SEM Analysis	96
4.3.4	FTIR Spectra Analysis	98
4.3.5	Optimum Irradiation Dose for the Curing of Natural Rubber/Clay Nanocomposites	100
4.3.6	Gel Content	102
4.3.7	Tensile Modulus of Natural Rubber/Clay Nanocomposites	104
4.3.8	Tensile Strength of Natural Rubber/Clay Nanocomposites	108

4.3.9	Elongation at Break of Natural Rubber/Clay Nanocomposites	109
4.3.10	Dynamic Mechanical Properties	111
4.3.11	Thermogravimetric Analysis	119
4.4	Preparation and Characterization of Poly(Ethylene-co-Vinyl Acetate)/Clay Nanocomposites	125
4.4.1	Structure Determination by X-Ray Diffraction	125
4.4.2	Transmission Electron Microscopy	128
4.4.3	Scanning Electron Microscopy Analysis	133
4.4.4	Degree of Crosslinking	135
4.4.5	Tensile Properties	137
4.4.6	Dynamic Mechanical Analysis	141
4.4.7	Thermogravimetric Analysis	146
4.5	Preparation and Characterization of NR/EVA/Clay Nanocomposites	152
4.5.1	X-ray Diffraction Study	152
4.5.2	Morphology Study by Transmission Elektron Microscopy	156
4.5.3	Scanning Electron Microscopy	165
4.5.4	Degree of crosslinking	167
4.5.5	Tensile Modulus	170
4.5.6	Tensile Strength	172
4.5.7	Elongation at Break	174
4.5.8	Dynamic Mechanical Analysis	176
4.5.9	Thermogravimetric Analysis	182
5.10	Flammability Property	190
5	CONCLUSION AND RECOMMENDATION FOR FUTURE WORK	192
5.1	Conclusion	192
5.2	Recommendation for Future Work	195
	REFERENCES/BIBLIOGRAPHY	197
	BIODATA OF THE AUTHOR	208

LIST OF TABLES

Table		Page
1.1	Chemical formula of commonly used 2:1 layered silicates	12
1.2	G_x and G_s value for various type of polymers	14
2.1	Tensile stress of nanocomposites	43
3.1	Amount of NR and organoclay used in preparing the nanocomposites	63
3.2	Amount of EVA and organoclay used in preparing the nanocomposites	64
3.3	Amount of NR, EVA and organoclay used in preparing the nanocomposites	65
4.1	2θ and interlayer distance of sodium montmorillonite and alkylammonium montmorillonites.	71
4.2	The carbon content and the amount of surfactant intercalated into the clay galleries from CHNS analysis	74
4.3	The amount of surfactant intercalated in the clay galleries obtained from TGA analysis	76
4.4	Tensile test results of NR/1CTA-MMT melt mixed at different temperatures and irradiated at 250 kGy	80
4.5	Tensile test results of NR/1CTA-MMT melt mixed at different rotor speeds and irradiated at 250 kGy	82
4.6	Tensile test results of NR/1CTA-MMT melt mixed at different mixing times and irradiated at 250 kGy	84
4.7	Storage modulus and glass transition temperatures of NR/DDA-MMT nanocomposites with different concentrations of DDA-MMT	115
4.8	Storage modulus and glass transition temperatures of NR and NR nanocomposites with 5 phr of different types of organoclay	118
4.9	Onset of degradation, maximum degradation temperature and weight of residue for NR/DDA-MMT nanocomposites	120



4.10	Onset of degradation, maximum degradation temperature and weight of residue for NR nanocomposites with 5 phr different type of organoclay	124
4.11	Maximum decomposition temperature and char yield of EVA/DDA-MMT nanocomposites before irradiation determine from TGA techniques	148
4.12	Maximum decomposition temperature and char yield of EVA/DDA-MMT nanocomposites after irradiation at 100 kGy determine from TGA techniques	151
4.13	Maximum decomposition temperature of NR/EVA/DDA-MMT nanocomposites before and after irradiation	185
4.14	Maximum decomposition temperature of NR/EVA/C20A nanocomposites before and after irradiation	188

LIST OF FIGURES

Figure		Page
1.1	Structure of polymer/clay nanocomposites	6
1.2	Structure of montmorillonite	10
2.1	Schematic illustration of formation of hydrogen bonds in Nylon-6/MMT nanocomposites	39
2.2	Proposed model for the fracture of (A) a glassy and (B) a rubbery polymer clay exfoliated nanocomposite with increasing strain	45
2.3	Formation of tortuous path in polymer/clay nanocomposites	57
4.1	XRD patterns of (a) Na-MMT, (b) DDA-MMT, (c) ODA-MMT, (d) CTA-MMT	71
4.2	FTIR spectra of Na-MMT, CTAB and CTA-MMT	73
4.3	FTIR spectra of Na-MMT, DDA-MMT, ODA-MMT and CTA-MMT	73
4.4	TGA thermograms of (a) Na-MMT, (b) DDA-MMT, (c) ODA-MMT and (d) CTA-MMT	75
4.5	DTG thermograms of (a) Na-MMT, (b) DDA-MMT, (c) ODA-MMT and (d) CTA-MMT	75
4.6	XRD patterns of NR/CTA-MMT melt mixed at different temperatures	79
4.7	XRD patterns of NR/CTA-MMT melt mixed at different rotor speeds	81
4.8	XRD patterns of NR/CTA-MMT at different mixing times	83
4.9	XRD patterns of Na-MMT and NR/Na-MMT composites	86
4.10	XRD patterns of DDA-MMT and NR/DDA-MMT nanocomposites	87
4.11	XRD patterns of ODA-MMT and NR/ODA-MMT nanocomposites	89

4.12	XRD patterns of CTA-MMT and NR/CTA-MMT nanocomposites	90
4.13	XRD patterns of C20A and NR/C20A nanocomposites	91
4.14	TEM micrographs of (a) NR/1CTA-MMT, (b) NR/3CTA-MMT, (c) NR/5CTA-MMT and (d) NR/10CTA-MMT nanocomposites at low magnification	92
4.15	TEM micrographs of (a) NR/1CTA-MMT, (b) NR/3CTA-MMT, (c) NR/5CTA-MMT and (d) NR/10CTA-MMT nanocomposites at high magnification	93
4.16	TEM micrographs of (a) NR/5Na-MMT, (b) NR/5DDA-MMT, (c) NR/5ODA-MMT, (d) NR/5CTA-MMT and (e) NR/5C20A nanocomposites at high magnification (25000x)	95
4.17	SEM micrographs of NR/10Na-MMT at low magnification	96
4.18	SEM micrographs of (a) NR/1DDA-MMT, (b) NR/3DDA-MMT, (c) NR/5DDA-MMT and (d) NR/10DDA-MMT at high magnification	97
4.19	Appearance of pure NR and NR filled with Na-MMT and DDA-MMT	98
4.20	FTIR spectra of Natural rubber and its nanocomposites with 1, 3, 5 and 10 phr DDA-MMT	99
4.21	Effect of irradiation dose on gel content of NR, NR/DDA-MMT and NR/ODA-MMT	100
4.22	Effect of irradiation dose on tensile strength of NR and NR/Clay nanocomposites	101
4.23	Gel content of NR/organoclay nanocomposites irradiated at 250 kGy	103
4.24	Modulus at 300% elongation of NR/Organoclay nanocomposites irradiated at 250 kGy	105
4.25	Stress strain curve of (a) NR, (b) NR/3DDA-MMT, (c) NR/5DDA-MMT and (d) NR/10DDA-MMT	107
4.26	Tensile strength of NR/Organoclay nanocomposites irradiated at 250 kGy	108
4.27	Elongation at break of NR/Organoclay nanocomposites irradiated at 250 kGy	110

4.28	Variation of storage modulus of NR/DDA-MMT nanocomposites as a function of temperature	113
4.29	Variation of $\tan \delta$ of NR/DDA-MMT nanocomposites as a function of temperature	114
4.30	Variation of storage modulus with temperature for (a) NR, (b) NR/5Na-MMT, (c) NR/5DDA-MMT, (d) NR/5ODA-MMT and (e) NR/5C20A	117
4.31	Variation of $\tan \delta$ with temperature for (a) NR, (b) NR/5NaMMT, (c) NR/5DDA-MMT, (d) NR/5ODA-MMT and (e) NR/5C20A	118
4.32	TGA thermograms of NR/DDA-MMT nanocomposites	119
4.33	DTG thermograms of NR/DDA-MMT nanocomposites	120
4.34	TGA thermograms of NR/organoclay nanocomposites	123
4.35	DTG thermograms of NR/organoclay nanocomposites	123
4.36	XRD patterns of (a) DDA-MMT, (b) EVA/1DDA-MMT, (c) EVA/3DDA-MMT, (d) EVA/5DDA-MMT and (e) EVA/10DDA/MMT	126
4.37	XRD patterns of (a) C20A, (b) EVA/1C20A, (c) EVA/3C20A, (d) EVA/5C20A and (e) EVA/10C20A	127
4.38	XRD patterns of Na-MMT and EVA/5Na-MMT composite	128
4.39	TEM micrographs of (a) EVA/1DDA-MMT, (b) EVA/3DDA-MMT, (c) EVA/5DDA-MMT and (d) EVA/10DDA-MMT at low magnification (4000x)	130
4.40	TEM micrographs of (a) EVA/1DDA-MMT, (b) EVA/3DDA-MMT, (c) EVA/5DDA-MMT and (d) EVA/10DDA-MMT at high magnification (25000x)	131
4.41	TEM micrographs of EVA/3C20A nanocomposite at low (4000x) and high (25000x) magnification	131
4.42	SEM micrographs of cryo-fractured surface of EVA/5Na-MMT (magnification 20000x)	133
4.43	SEM micrographs of cryo-fractured surface of (a) EVA/1DDA-MMT, (b) EVA/3DDA-MMT, (c) EVA/5DDA-MMT and (d) EVA/10DDA-MMT (magnification 20000x)	134

4.44	Gel content of EVA/DDA-MMT and EVA/5C20A irradiated at different doses	135
4.45	Gel content of EVA/clay nanocomposites irradiated at 100 kGy	136
4.46	Modulus at 300% elongation of EVA/DDA-MMT and EVA/C20A before and after irradiation at 100 kGy	138
4.47	Tensile strength of EVA/DDA-MMT and EVA/C20A before and after irradiation at 100 kGy	140
4.48	Elongation at break of EVA/DDA-MMT and EVA/C20A before and after irradiation at 100 kGy	141
4.49	Storage modulus of (a) EVA, (b) EVA/5DDA-MMT and (c) EVA/10DDA-MMT nanocomposites before irradiation	142
4.50	Storage modulus of (a) EVA, (b) EVA/5DDA-MMT and (c) EVA/10DDA-MMT nanocomposites irradiated at 100 kGy	143
4.51	Storage modulus of (a) EVA, (b) EVA/5C20A and (c) EVA/10C20A nanocomposites irradiated at 100 kGy	143
4.52	Tan δ of (a) EVA, (b) EVA/5DDA-MMT and (c) EVA/10DDA-MMT nanocomposites before irradiation	145
4.53	Tan δ of (a) EVA, (b) EVA/5DDA-MMT and (c) EVA/10DDA-MMT nanocomposites irradiated at 100 kGy	145
4.54	Tan δ of (a) EVA, (b) EVA/5C20A and (c) EVA/10C20A irradiated at 100 kGy	146
4.55	TGA thermograms of EVA/DDA-MMT nanocomposites	147
4.56	DTG thermograms of EVA/DDA-MMT nanocomposites	147
4.57	TGA thermograms of pure EVA, EVA/3DDA-MMT and EVA/3C20A	150
4.58	DTG thermograms of pure EVA, EVA/3DDA-MMT and EVA/3C20A	150
4.59	X-ray diffraction patterns of Na-MMT and NR/EVA/Na-MMT composites	153

4.60	X-ray diffraction patterns of DDA-MMT and NR/EVA/DDA-MMT nanocomposites	154
4.61	X-ray diffraction patterns of C20A and NR/EVA/C20A nanocomposites	155
4.62	TEM micrographs at low magnification (4000x) of (a) NR/EVA/5Na-MMT, (b) NR/EVA/5DDA-MMT and (c) NR/EVA/5C20A	157
4.63	TEM micrographs at low magnification (4000x) of (a) NR/EVA/1DDA-MMT, (b) NR/EVA/3DDA-MMT (c) NR/EVA/5DDA-MMT and (d) NR/EVA/10DDA-MMT	159
4.64	TEM micrographs at high magnification (10000x) of (a) NR/EVA/1DDA-MMT, (b) NR/EVA/3DDA-MMT, (c) NR/EVA/5DDA-MMT and (d) NR/EVA/10DDA-MMT	160
4.65	TEM micrographs at high magnification (25000) of (a) NR/EVA/1DDA-MMT, (b) NR/EVA/3DDA-MMT, (c) NR/EVA/5DDA-MMT and (d) NR/EVA/10DDA-MMT	161
4.66	TEM micrographs at low magnification (4000x) of (a) NR/EVA/1C20A, (b) NR/EVA/3 C20A, (c) NR/EVA/ 5C20A and (d) NR/EVA/ 10C20A	162
4.67	TEM micrographs at high magnification (10000x) of (a) NR/EVA/1C20A, (b) NR/EVA/3 C20A, (c) NR/EVA/5C20A and (d) NR/EVA/10C20A	163
4.68	TEM micrographs at high magnification (25000x) of (a) NR/EVA/1C20A, (b) NR/EVA/3 C20A, (c) NR/EVA/5C20A and (d) NR/EVA/10C20A	164
4.69	SEM micrographs of cryo-fractured surface of (a) NR/EVA, (b) NR/EVA/5Na-MMT, (c) NR/EVA/5DDA-MMT and (d) NR/EVA/5C20A	166
4.70	SEM micrographs of (a) NR/EVA, (b) NR/EVA/5Na-MMT, (c) NR/EVA/5DDA-MMT and (d) NR/EVA/5C20A treated with toluene	167
4.71	The relationship between gel content and irradiation doses	168
4.72	Gel content vs. clay content of NR/EVA/organoclay nanocomposites irradiated at 150kGy	169
4.73	Modulus at 300% elongation of NR/EVA/clay nanocomposites at various clay content before and after irradiation at 150 kGy	170

4.74	Tensile strength of NR/EVA/clay nanocomposites at various clay content before and after irradiation at 150 kGy	172
4.75	Elongation at break of NR/EVA/clay nanocomposites at various clay content before and after irradiation at 150 kGy	175
4.76	Storage modulus of (a) NR/EVA, (b) NR/EVA/3DDA-MMT, (c) NR/EVA/5DDA-MMT and (d) NR/EVA/10DDA-MMT	177
4.77	Tangent delta of (a) NR/EVA, (b) NR/EVA/3DDA-MMT, (c) NR/EVA/5DDA-MMT and (d) NR/EVA/10DDA-MMT	177
4.78	Storage modulus of (a) NR/EVA, (b) NR/EVA/5C20A and (c) NR/EVA/10C20A	179
4.79	Tangent δ of (a) NR/EVA, (b) NR/EVA/5C20A and (c) NR/EVA/10C20A	180
4.80	Storage modulus of (a) NR/EVA/5DDA-MMT at 0 kGy and (b) NR/EVA/5DDA-MMT at 150 kGy	181
4.81	Tangent δ of (a) NR/EVA/5DDA-MMT at 0 kGy and (b) NR/EVA/5DDA-MMT at 150 kGy	182
4.82	Thermogravimetric analysis of unfilled NR/EVA blend.	183
4.83	TGA thermograms of NR/EVA/DDA-MMT nanocomposites	184
4.84	DTG thermograms of NR/EVA/DDA-MMT nanocomposites	184
4.85	TGA thermograms of NR/EVA/C20A nanocomposites	188
4.86	DTG thermograms of NR/EVA/C20A nanocomposites	188
4.87	TGA thermograms of NR/EVA, NR/EVA/Na-MMT and NR/EVA/5DDA-MMT	189
4.88	DTG thermograms of NR/EVA, NR/EVA/Na-MMT and NR/EVA/5DDA-MMT	189
4.89	Limiting oxygen index of NR/EVA/C20A nanocomposites	191

LIST OF SYMBOLS AND ABBREVIATIONS

Å	Amstrong
APP	Ammonium polyphosphate
bsg	Bahagian seratus getah
C18	Octadecylammonium
C18-MMT	Octadecyl ammonium montmorillonite
C20A	Cloisite 20A
C30B	Methyl-tallow-bis-2-hydroxyethyl quaternary ammonium montmorillonite
C6A	Dimethyl dihydrogenated tallow ammonium montmorillonite.
CEC	Cation exchange capacity
CHNS	Carbon, hydrogen, nitrogen and sulfur
CTA-MMT	Cetyltrimethyl ammonium montmorillonite
DDA-MMT	Dodecyl ammonium montmorillonite
DIOM	Diocadecyl dimethyl ammonium montmorillonite
DMA	Dynamic mechanical analysis
DMDS-MMT	dimethyl distearyl ammonium bromide modified MMT
DSC	Differential scanning calorimetry
DTG	Derivative thermogravimetric
EB	Electron beam
Eb	Elongation at break
ENR	Epoxidized natural rubber
EPDM	Ethylene-propylene-diene monomer
EVA	Poly (ethylene-co-vinyl acetate)